Sensors and Materials, Vol. 35, No. 9 (2023) 1–11
MYU Tokyo

S & M ####

Accuracy Assessment of Google Earth and Open-source Digital Elevation Models in China Using GPS on Field Control Points

Xuwan Zhang,[1] Lei You,[1] Mingjun Deng,[1*] Yuan Kou,[2] and Yin Yang[3]

[1]School of Automation and Electronic Information, Xiangtan University, Xiangtan 411105, China
[2]The First Surveying and Mapping Institute of Hunan Province, Changsha, China
[3]School of Mathematics and Computational Science, Xiangtan University, Xiangtan 411105, China

(Received March 9, 2023; accepted July 4, 2023)

Keywords: AW3D30, Google Earth, horizontal accuracy, TanDEM-X, vertical accuracy

Google Earth (GE) provides accurate and reliable global high-resolution images and can obtain the coordinates of any point on Earth's surface. A digital elevation model (DEM) is a dataset that quantitatively reflects the elevation of Earth's surface. Although GE and DEMs can be used to obtain the coordinates of any position on Earth, their open-access data can be affected by various factors, thereby inducing undesirable precision variability. Therefore, it is essential to estimate the accuracy of GE and open-source DEMs. In this study, 325 high-precision GPS survey points in 16 regions in China were used to evaluate the horizontal and vertical accuracies of GE and the elevation accuracy of two open-source DEMs. GE had a high horizontal accuracy with a root mean square error (*RMSE*) of 2.495 m and an error range of 1.090–4.844 m. The elevation accuracy of GE (*RMSE* = 2.610 m) was lower than those of TanDEM-X (*RMSE* = 2.055 m) and AW3D30 (*RMSE* = 2.373 m) DEMs. At the same time, the impacts of slope, aspect, and feature type on the accuracy of these data are studied and analyzed. The results show that the accuracy of control data are closely related to the characteristics of the study area. Overall, these findings indicate that for future studies in China, GE can be used to acquire horizontal data, whereas TanDEM-X and AW3D30 are more suitable for elevation data that have higher precision and provide a reference for relevant research on geographic information.

1. Introduction

The determination of geodetic coordinates (longitude, latitude, and elevation) of any target on Earth is of the utmost significance in military, aviation, navigation, surveying, mapping, and other applications. Although the global navigation satellite system provides an efficient way to obtain the spatial position of a given target, it requires the target to have a receiving terminal. Therefore, it can only obtain the position of a cooperative target (one having a receiving terminal), which has limitations. As Google Earth (GE), AW3D30, TanDEM-X, and other open-source digital elevation model (DEM) data can provide the spatial location of non-cooperative

*Corresponding author: e-mail: xtudmj@xtu.edu.cn

ISSN 0914-4935

targets over a wide range, they each have recently attracted considerable attention.[1]

GE, a virtual Earth software program originally developed by Google in 2005, arranges satellite photographs, aerial photographs, and geographic information system data on a three-dimensional model of Earth at a global scale. However, Google has not officially reported its accuracy.

In contrast, a DEM is a digital expression of the surface morphology, reflecting the terrain and geomorphology information necessary for the application and analysis of geography. DEMs are a cornerstone of modern studies on geography, geomorphology, and geographic information. Their reliability and accuracy are directly related to the efficiency of the application itself. The low precision of GE or DEM open-source services would introduce adverse effects when applied to the high-precision positioning task of a target.[2] Therefore, to provide a reference for users, an evaluation of the accuracy of GE and DEM data is urgently needed.

GE can provide plane and elevation information of a target, many global DEMs can provide elevation information, and many scholars have evaluated its accuracy. For instance, Benker *et al.* evaluated the accuracy of GE in the Big Bend area in Texas, USA and revealed a horizontal accuracy of 2.64 m and a root mean square error (*RMSE*) of the vertical accuracy of 1.63 m. However, the authors still urge caution when using the GE Terrain Model to extract remote sensing research data.[3] Furthermore, Farah and Algarni used differential static GPS technology to evaluate the horizontal and vertical accuracies of GE in the Riyadh area, the capital of the Kingdom of Saudi Arabia. They reported *RMSE* estimates in the horizontal and vertical directions of 2.18 m and 1.51 m, respectively.[2] Mohammed *et al.* evaluated the horizontal and vertical accuracies of GE in Khartoum using GPS technology, thus revealing *RMSE*s in the horizontal and vertical directions of 1.59 m and 1.7 m, respectively.[4] El Ashmawy selected approximately 200 points in the Dabaa region on the northern coast of Egypt and evaluated the vertical accuracy of GE. He showed that the *RMSE* in the vertical direction was 1.85 m, thus indicating that GE had high accuracy in the vertical direction.[5] In 2020, Guo *et al.*, taking typical regions in Asia as research objects, used statistical analysis methods to verify the horizontal accuracy of GE and purchased WorldView (WV) data. The results show that the accuracy evaluation may be affected by the terrain features and unimportant feature points in the study area.[6]

A DEM can also provide elevation information for a target; therefore, evaluating its accuracy is essential. Li *et al.* selected five samples of typical terrain in China to evaluate the vertical accuracies of the AW3D30 and SRTM DEMs. They found that AW3D30 had a high vertical accuracy, with a *RMSE* of 4.81 m. At the same time, it was found that the terrain slope and the type of features jointly affect the vertical accuracy of AW3D30, and the former may have a greater impact than the latter.[7] Li *et al.* utilized GPS observation data, selecting the Wenchuan, Three Gorges, and Qingdao regions in China to evaluate the vertical accuracies of the ASTER GDEM, SRTM, NASADEM, and TanDEM-X 90 m DEMs. They found the overall performance of TanDEM-X to be better than those of other global DEMs.[8] Han *et al.* selected four 1 × 1° tile areas in China (Sichuan, Xinjiang A, Xinjiang B, and Inner Mongolia) to evaluate the accuracy of these areas and found that TanDEM-X exhibited the best comprehensive quality, followed by SRTM.[9] Vassilaki and Stamos selected 14 stations in Europe, the United States, and Antarctica

to evaluate the vertical accuracies of AW3D30, ASTER, SRTM1, and SRTM3. They demonstrated that the *RMSE* of TanDEM-X in the vertical direction was 1.0–8.7 m, whereas that of AW3D30 was 2.6–49.0 m.[10] Taking Hunan Province in China as an example, Liu *et al.* found that the accuracy of DEMs decreased with increasing terrain elevation and slope, whereas the error of DEM was independent of the terrain slope. As the land cover type changes from vegetation to non-vegetation, the accuracy will improve.[11] Overall, research on the accuracies of GE and DEM data is limited, and their accuracy evaluations are somewhat isolated. Moreover, in China, most studies have focused on a specific region or the same data type; therefore, a large-scale and holistic study on this topic is lacking. To address this problem, we selected 16 research areas in China to evaluate the horizontal and vertical accuracies of GE and the elevation accuracies of two mainstream open-source DEMs (TanDEM-X and AW3D30).

2. Data and Methods

2.1 Study area

Sixteen regions in China were selected (Fig. 1). These regions were bounded latitudinally from Zhangye, Gansu (39° N) to Wenchang, Hainan (19° N), and longitudinally from Ningbo, Zhejiang (122° E) to Zhangye, Gansu (100° E). The survey area was wide and included northwest, southwest, north, east, south, and central China.

2.2 Experimental data

2.2.1 GE

GE images of the 16 study areas were obtained, where SRTM was used as the elevation data source. The internal horizontal coordinate system of GE was determined using the 1984 World

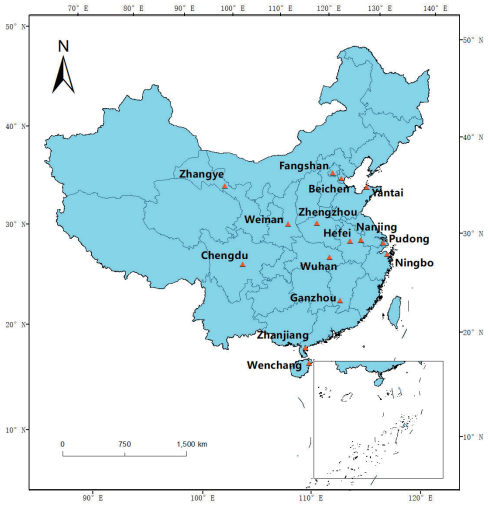

Fig. 1. (Color online) Study area.

Geodetic System (WGS84). Its vertical component was determined in accordance with the WGS84-EGM96 geoid vertical datum.[4]

2.2.2 DEM

Several open-source DEMs, including AW3D30, TanDEM-X, SRTM, and ASTER, are available. As TanDEM-X and AW3D30 have the best accuracies, we selected these two DEMs to evaluate the accuracy of GE.

TanDEM-X: TanDEM-X was a cooperative project between the German Aerospace Research Center (DLR) and Astrium (EADS) from 2010 to 2015. As with SRTM, the elevation data were obtained by synthetic aperture radar (SAR) interferometry. In this study, the images were retrieved using a dual satellite system consisting of the TerraSAR-X and TanDEM-X satellites. The TerraSAR-X satellite was launched in June 2007, and the TanDEM-X satellite was launched in June 2010. The two satellites flew in a tight spiral formation. Since September 2016, the new TanDEM-XDEM has been deemed to be one of the most consistent, highly accurate, and complete global DEM datasets of Earth's surface.[12] The horizontal datum plane of TanDEM-X is WGS84-G1150, and the height refers to the ellipsoidal height of WGS84-G1150.[13]

AW3D30: The ALOS Global Digital Surface Model (DSM) "ALOSWold3D-30m" is a high-precision global digital terrain model DSM made freely available by the Japan Aerospace Exploration Agency in May 2016; it has a horizontal resolution of 30 m (1 arcsecond) and is generated from images with a resolution of 5 m. The AW3D30 DEM was developed using millions of images acquired using a panchromatic optical sensor (PRISM) on the ALOS satellite.[14] The first version of AW3D30 was released in May 2016, and new versions have been successively released. The latest version improves the absolute and relative accuracies through additional calibration and gap filling. The coordinate systems used by AW3D30 are WGS84 (horizontal coordinate system) and WGS84-EGM96 geoid (vertical coordinate system).[15]

2.3 Reference data

Approximately 20 GPS control points [Fig. 2(a)] were selected at 10 km intervals in each study area, giving a total of 325 control points; these were mainly cross-shaped [Figs. 2(b)–2(c)] or T-shaped road centers and other points that were easy to distinguish and identify. At each control point, the continuous operation (satellite positioning service) reference station (CORS) established by the multi-base station network RTK technology was adopted for precision measurement, and the horizontal and vertical point location measurements were better than 0.1 m.[16]

2.4 Research method

2.4.1 Data processing

Horizontal accuracy: The WGS84 coordinate system was utilized in this study. We located the positions of 325 control points in GE. The positions of the GPS control points obtained in GE

(a) (b) (c)

Fig. 2. (Color online) Examples of reference data: (a) distribution of control points in Chengdu, Sichuan, (b) site survey of Site 173101063 in Pudong District, Shanghai, and (c) position of point 173101063 in GE.

and the real measured positions of GPS control points were transformed into Universal Transverse Mercator Projection (UTM) plane projection coordinates. The horizontal accuracy of the image was evaluated using the *RMSE*s *RMSEx*, *RMSEy*, and *RMSEr* in the east–west, north–south, and horizontal directions, respectively.

$$RMSEx = \sqrt{\frac{\sum_i \left(x_{data,i} - x_{reference,i}\right)^2}{n}} \tag{1}$$

$$RMSEy = \sqrt{\frac{\sum_i \left(y_{data,i} - y_{reference,i}\right)^2}{n}} \tag{2}$$

$$RMSEr = \sqrt{RMSEx^2 + RMSEy^2} \tag{3}$$

$x_{data,i}$ is the coordinate of the ith control point in GE, $x_{reference,i}$ is the east–west UTM coordinate of the ith control point in the east–west UTM coordinate system measured by GPS-RTK technology, $y_{data,i}$ is the coordinate of the ith control point in GE in the north–south UTM coordinate system, $y_{reference,i}$ is the coordinate of the ith control point in the north–south UTM coordinate system measured by GPS-RTK technology, n is the number of reference points, and i represents an integer from 1 to n.

Vertical accuracy: EGM96 was used as the vertical datum plane for GE and AW3D30, whereas WGS84-G1150 was used for the TanDEM-X and GPS control points. To ensure the comparability of the datum, it was necessary to convert it into a uniform vertical datum. The WGS84 ellipsoid was used as the vertical datum, and the EGM96 geoid correction model was added to AW3D30 and GE to achieve the unification of the elevation data. The vertical accuracy of the data was evaluated using the *RMSE* and mean error (*ME*) in the vertical direction.

$$\Delta h = h_{data} - h_{reference} \tag{4}$$

$$ME = \frac{\sum_i \Delta h}{n} \tag{5}$$

$$RMSE = \sqrt{\frac{\sum_i \Delta h^2}{n}} \tag{6}$$

h_{data} is the elevation obtained through the relevant open-source DEM data source, $h_{reference}$ is the true elevation measured by GPS-RTK technology, Δh is the difference between the obtained elevation and the true value measured by GPS, n is the number of reference points, and i represents an integer from 1 to n.

2.4.2 Research program

The research scheme included the following: (1) descriptive statistics of GE horizontal accuracy, and (2) descriptive statistics of GE, TanDEM-X, and AW3D30 vertical accuracies; (3) descriptive statistical analysis of surface ground coverage types; (4) descriptive statistical analysis of slope and aspect effects.

3. Results

3.1 Overall accuracy evaluation

3.1.1 GE horizontal accuracy

Statistical analysis was applied to the spatial resolution of the study area. In this context, *RMSE* was measured separately in the horizontal direction of each study area. The *RMSEx* range in the east–west direction was 0.693–4.375 m (Table 1). The minimum error was obtained in the Hefei region, whereas the maximum error was noted in the Zhangye region. The *RMSE*y range in the north–south direction was 0.367–3.256 m. The minimum error was identified in Hefei, whereas the maximum error was identified in Wenchang. The overall *RMSEx*, *RMSEy*, and *RMSEr* were 1.927, 1.586, and 2.495 m, respectively, indicating that the GE horizontal data are highly accurate in China.

3.1.2 Vertical accuracy

Statistical analysis of regional data (Table 2) showed that the *RMSE*s of GE and the two DEMs mostly varied by ~2 m. TanDEM-X exhibited the weakest variability, followed by AW3D30 and GE (Fig. 3). Analysis of GE data revealed that Fangshan (0.768 m) and Wenchang (6.375 m) had the smallest and largest vertical *RMSE* values, respectively. Analysis of *RMSE* in

Table 1
GE horizontal direction error measurements. Error items include: east–west RMSE (*RMSEx*), north–south RMSE (*RMSEy*), and horizontal RMSE (*RMSEr*) in the UTM coordinate system; unit = *m*.

Study Area	*RMSEx*	*RMSEy*	*RMSEr*	Study Area	*RMSEx*	*RMSEy*	*RMSEr*
Fangshan	2.179	2.339	3.196	Zhengzhou	1.331	2.158	2.535
Beichen	2.647	2.062	3.355	Hefei	0.693	0.367	0.784
Weinan	1.165	1.373	1.801	Wuhan	2.945	1.611	3.357
Zhangye	4.375	2.079	4.844	Ganzhou	2.647	2.062	3.355
Yantai1	0.747	1.456	1.636	Chengdu	0.901	1.424	1.685
Yantai2	1.405	1.871	2.339	Zhanjiang	1.017	1.364	1.701
Pudong	1.548	1.291	2.016	Wenchang	3.068	3.256	1.09
Nanjing	1.034	1.047	1.471	Ningbo	1.457	0.965	1.747
Overall	1.927	1.586	2.495				

Table 2
Measurement of vertical error of selected data sources in 16 study areas. Error items include *ME* and *RMSE*; unit = *m*.

Study Area	Source	*ME*	*RMSE*	Study Area	Source	*ME*	*RMSE*
	AW3D30	2.028	2.306		AW3D30	0.939	1.334
Fangshan	TanDEM-X	0.524	1.663	Zhengzhou	TanDEM-X	−0.728	1.523
	GE	0.508	0.768		GE	0.967	1.587
	AW3D30	0.085	1.621		AW3D30	0.76	1.441
Beichen	TanDEM-X	0.042	1.257	Hefei	TanDEM-X	−0.821	1.712
	GE	−0.937	1.217		GE	0.809	1.212
	AW3D30	−2.093	2.749		AW3D30	3.54	5.051
Weinan	TanDEM-X	−0.45	1.516	Wuhan	TanDEM-X	2.06	3.182
	GE	−1.129	6.375		GE	−1.446	1.529
	AW3D30	−0.563	1.676		AW3D30	1.117	3.24
Zhangye	TanDEM-X	−1.829	1.994	Ganzhou	TanDEM-X	0.575	3.54
	GE	1.271	1.692		GE	−2.442	4.048
	AW3D30	−1.554	2.134		AW3D30	0.658	1.094
Yantai1	TanDEM-X	0.333	1.979	Chengdu	TanDEM-X	−0.118	0.889
	GE	−0.972	1.353		GE	−0.859	1.617
	AW3D30	0.244	1.788		AW3D30	−2.301	2.656
Yantai2	TanDEM-X	0.924	2.46	Zhanjiang	TanDEM-X	−0.74	1.434
	GE	0.823	2.454		GE	−0.492	3.005
	AW3D30	1.127	1.993		AW3D30	−0.582	2.209
Pudong	TanDEM-X	1.123	1.714	Wenchang	TanDEM-X	1.362	2.843
	GE	1.397	2.420		GE	0.279	3.915
	AW3D30	1.168	2.015		AW3D30	1.292	2.841
Nanjing	TanDEM-X	−0.163	0.935	Ningbo	TanDEM-X	0.563	2.207
	GE	−1.753	1.925		GE	−1.333	1.493
	AW3D30	−0.233	2.373				
Overall	TanDEM-X	0.397	2.055				
	GE	0.220	2.610				

the vertical direction for all the study areas demonstrated that TanDEM-X had the highest accuracy (*RMSE* = 2.055 m), followed by AW3D30 (*RMSE* = 2.373 m) and GE (*RMSE* = 2.610 m).

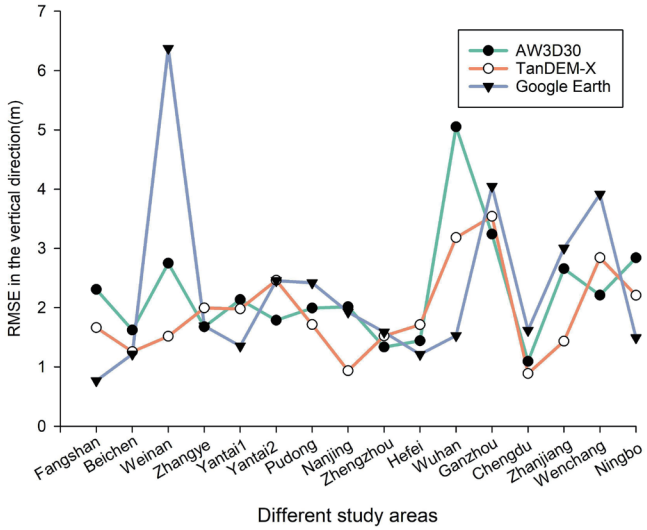

Fig. 3. (Color online) *RMSE* in the vertical direction for GE, AW3D30, and TanDEM-X in all study areas.

3.2 Analysis of factors affecting accuracy

3.2.1 Ground coverage type

When analyzing the impact of surface feature coverage type on the accuracy of 3D control data, the global 10-meter-resolution surface feature coverage type data released by a Tsinghua University team in 2017 was used. The research area of this experiment comprised cultivated land and artificial surface. Therefore, only the impacts of these two types of surface cover types were analyzed (Table 3).

The type of surface cover changed from cultivated land to artificial surface, and the *RMSE* in the east–west, north–south, and horizontal directions increased. It increased by 0.328 m in the east–west direction, 0.348 m in the north–south direction, and 0.475 m in the overall horizontal direction (Fig. 4). In the vertical direction, the *RMSE* of GE decreased (1.001 m), the *RMSE* of AW3D30 increased (0.693 m), and the *RMSE* of TanDEM-X increased (0.334 m) (Fig. 5).

3.2.2 Slope and aspect

In this study, the slope of the GPS points measured in the 16 study areas is less than 5°. Therefore, it can be regarded as a control variable when studying the effects of slope and aspect on the accuracy of 3D control data. By the control variable method, we analyzed only the impact of slope aspect on data accuracy. The slope aspect is from 0 to 360°, divided into 8 ranges (Table 4). The effect of slope aspect on various data *ME* was analyzed.

Next, the *ME* radar images from three data sources and five different directions in all the study areas were analyzed in terms of the slope direction (Fig. 6). The radar images in the vertical direction of AW3D30 and the north–south direction of GE are closest to the octagonal

Table 3
Ground coverage type of the study area.

Land cover type	Cropland	Artificial surface
Land cover class	1	6
Number of points	151	166

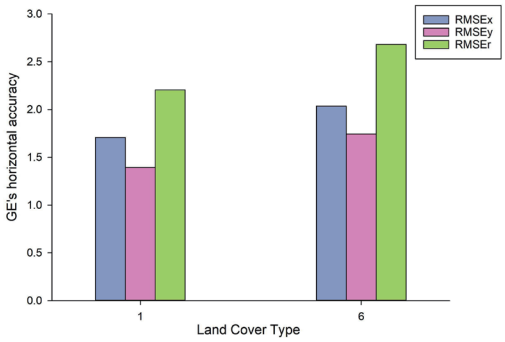

Fig. 4. (Color online) Three directions of GE histogram classified by the type of ground cover in all study areas: east–west direction, north–south direction, and horizontal direction.

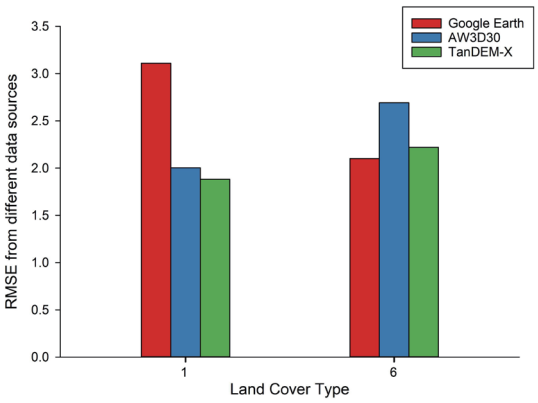

Fig. 5. (Color online) Histograms of the vertical directions of three data sources classified by the type of ground cover in all study areas: GE, AW3D30, TanDEM-X.

Table 4
Slope aspect classification in this study.

Azimuth (°)	Aspect
337.5–22.5	N
22.5–67.5	NE
67.5–112.5	E
112.5–157.5	SE
157.5–202.5	S
202.5–247.5	SW
247.5–292.5	W
292.5–337.5	NW

shape, and the radar images in other directions also approximate the octagonal shape. Within the allowable range of error, the slope direction has little influence on the north–south longitude accuracy of GE, and the vertical accuracies of GE, AW3D30, and TanDEM-X can be ignored if the accuracy requirement is not high. For GE in the vertical direction, *ME* values are overestimated in the N and E directions, but underestimated in other directions. The *ME* value of AW3D30 is overestimated in eight slope directions, of which the maximum overestimated value of slope W is 1.068 m, and the minimum overestimated value of slope S is 0.135 m. In the vertical direction of TanDEM-X and the south–north direction of GE, *ME* is overvalued and undervalued with a relatively average slope direction, respectively. In general, GE is undervalued in the east–west direction and overvalued in other directions.

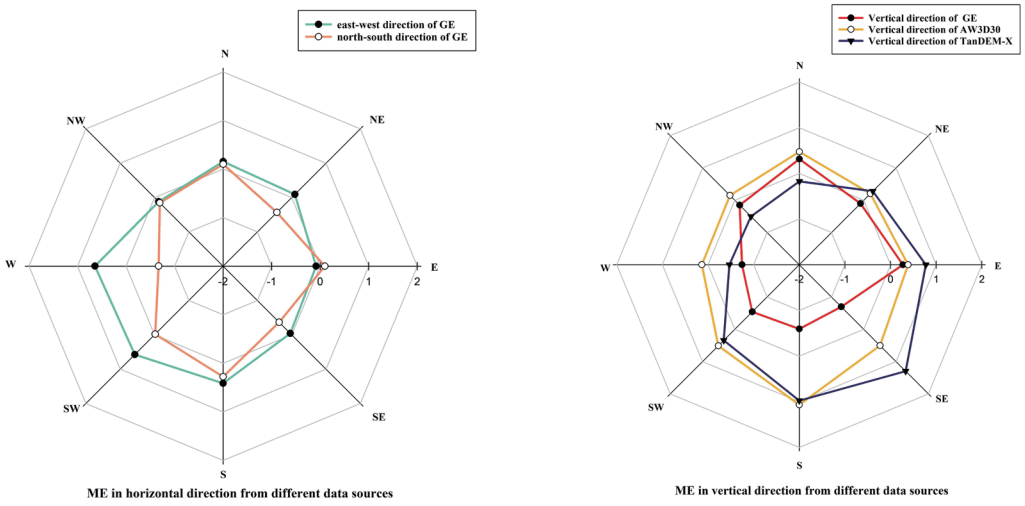

(a) (b)

Fig. 6. (Color online) *ME* radar images of (a) GE in the east–west and north–south directions and (b) GE, AW3D30, and TanDEM-X in the vertical direction classified by slope direction, for all study areas.

4. Conclusions

In this study, the accuracies of GE, AW3D30, and TanDEM-X in 16 regions in China were evaluated using GPS survey points. Overall, the horizontal *RMSE* of GE in China is 2.495 m; this is similar to the 2.64 m measured by Benker *et al.* in the Big Bend region, Texas, USA. There was a small difference in the *RMSE* between the east–west and north–south directions under the UTM coordinate system. Moreover, the east–west direction accuracy was slightly higher than that in the north–south direction. TanDEM-X stands out as having the highest vertical accuracy (*RMSE* = 2.055 m), followed by AW3D30 (*RMSE* = 2.373 m) and GE (*RMSE* = 2.610 m).

At the same time, the figure coverage type also affects the accuracy of 3D control data. When slope is considered as a control variable, the impact of the slope aspect on the accuracy cannot be ignored. When the type of ground cover changes from cultivated land to artificial surface, the accuracy of GE in the north–south direction decreases, and the horizontal variance increases, and the influence of the east–west direction becomes relatively small. In the vertical direction, the error of GE decreases significantly, the error of AW3D30 increases, and the error of TanDEM-X increases slightly. Therefore, the change in ground cover type in this study has the smallest and most stable effect on TanDEM-X in the vertical direction.

The horizontal GE data and TanDEM-X elevation data can be used to select 3D control data for geographic-information-related research in China, thereby improving the accuracy of the corresponding results.

Acknowledgments

This work was supported by National Key Research and Development Program of China (Grant No. 2020YFA0713503) and the Excellent Youth Project of the Hunan Provincial Education Department (Grant No. 22B0168).

References

1 S. Shetty, P. C. Vaishnavi, P. Umesh, and A. Shetty: Modell. Earth Syst. Environ. **8** (2022) 883. https://doi.org/10.1007/s40808-021-01119-2
2 A. Farah and D. Algarni: Artif. Satell. **49** (2014) 101. https://doi.org/10.2478/arsa-2014-0008
3 S. C. Benker, R. P. Langford, and T. L. Pavlis: Geocarto Int. **26** (2011) 291. https://doi.org/10.1080/10106049.2011.568125
4 N. Z. Mohammed, A. Ghazi, and H. E. Mustafa: Int. J. Multidiscip. Sci. Engineer. **4** (2013) 6. https://www.ijmse.org/Volume4/Issue6.html
5 K. L. A. El-Ashmawy: Artif. Satell. **51** (2016) 89. https://doi.org/10.1515/arsa-2016-0008
6 J. Guo, J. Zhang, H. Zhao, C. Li, J. Zhou, H. Tu, and Y. Zhao: Int. Arch. Photogramm. Remote Sens. Spatial Inf. Sci. XLIII-B3 (2020) 1333. https://doi.org/10.5194/isprs-archives-XLIII-B3-2020-1333-2020
7 H. Li and J. Zhao: IEEE J-STARS. **11** (2018) 4430. https://doi.org/10.1109/JSTARS.2018.2874361
8 P. Li, Z. Li, K. Dai, Y. Al-Husseinawi, W. Feng, and H. Wang: IEEE J. Sel. Top. Appl. Earth Obs. Remote Sens. **14** (2021) 5152. https://doi.org/10.1109/JSTARS.2021.3073782
9 H. Han, Q. Zeng, and J. Jiao: Remote Sens. **13** (2021) 1304. https://doi.org/10.3390/rs13071304
10 D. I. Vassilaki and A. A. Stamos: ISPRS J. Photogramm. Remote Sens. **160** (2020) 33. https://doi.org/10.1016/j.isprsjprs.2019.11.015
11 Z. Liu, J. Zhu, H. Fu, C. Zhou, and T. Zuo: Sensors **20** (2020) 4865. https://doi.org/10.3390/s20174865
12 Wessel, M. Huber, C. Wohlfart, U. Marschalk, D. Kosmann, and A. Roth: ISPRS J. Photogramm. Remote Sens. **139** (2018) 171. https://doi.org/10.1016/j.isprsjprs.2018.02.017
13 K. Gdulová, J. Marešová, and V. Moudrý: Remote Sens. Environ. **241** (2020) 111724. https://doi.org/10.1016/j.rse.2020.111724
14 Fazilova, K. Magdiev, and L. Sichugova: Int. J. Geoinformatics **1** (2021) 19. https://doi.org/10.52939/ijg.v17i1.1701
15 T. D. Acharya, I. T. Yang, and D. H. Lee: J. Korean Soc. Surv. Geod. **36** (2018) 17. https://doi.org/10.7848/KSGPC.2018.36.1.17
16 Q. Wu, J. Kang, S. Li, J. Zhen, and H. Li: Sensors **15** (2015) 30419. https://doi.org/10.3390/s151229806